Viscosity and surface-free energy effects in thermal shrinking of solid-state nanopores

Joseph A. Billo,[1,2,3] Jared Jones,[2,3,4] Waseem Asghar,[1,2,3] Ronald L. Carter,[1] and Samir M. Iqbal[1,2,3,4,5,a)]

[1]*Department of Electrical Engineering, University of Texas at Arlington, Arlington, Texas 76011, USA*
[2]*Nanotechnology Research and Teaching Facility, University of Texas at Arlington, Arlington, Texas 76019, USA*
[3]*Nano-Bio Lab, University of Texas at Arlington, Arlington, Texas 76019, USA*
[4]*Department of Bioengineering, University of Texas at Arlington, Arlington, Texas 76010, USA*
[5]*Joint Graduate Committee of Bioengineering Program, University of Texas at Arlington and University of Texas Southwestern Medical Center at Dallas, University of Texas at Arlington, Arlington, Texas 76010, USA*

(Received 27 March 2012; accepted 24 April 2012; published online 5 June 2012)

Solid-state nanopores are fabricated by either drilling these in thin membranes or by shrinking large pores with electron/ion beam. Simple heating of thin membranes with many large pores has been shown recently to controllably shrink these to nanoscale in parallel. Thermal heating of solid membrane in furnace changes the physical material properties. A model for the experimental nanopore shrinking data is developed. The parametric variations of viscosity, movement of adatoms and diffusion coefficients at temperature points around 1000 °C are characterized. The model provides a framework to understand and predict thermal shrinking of nanopores. © *2012 American Institute of Physics*. [http://dx.doi.org/10.1063/1.4725515]

Interest in solid-state nanopores followed the application of α-hemolysin protein nanopores as biosensors. Like protein nanopores, solid-state nanopores can provide single molecule analysis of proteins and DNA.[1–6] However, solid-state nanopores have been shown to be more robust than protein nanopores and are able to withstand different environmental conditions (*p*H, temperature, salinity, etc.).[7,8] In order for a solid-state nanopore to function as a biosensor, the diameter has to be about the same size as a single molecule of the analyte it is designed to detect. This small nano-scale diameter allows the biomolecule to cause significant current blockage in the ionic current as it electrophoretically passes through the nanopore. In recent years, a number of approaches have been reported to fabricate solid-state nanopores.[9–15] Most of these involve drilling nanopores using tightly focused electron or ion beams or creating nanopores initially much larger than the final desired size and then shrinking these using focused beams in transmission/scanning electron microscopes (TEM/SEM) or focused ion beam (FIB).[10,13] All of these methods process one nanopore die at a time and many times change the chemical composition of the nanopore material as well. These result in changes in the nanopore surface properties which in turn produce increased electrical noise and hamper the molecular analysis at low trans-membrane bias.

We recently reported an approach for shrinking nanopores in a thermal oxidation furnace.[16] The process involved initial creation of a 100 to 300 nm diameter nanopore in a 300 nm thick SiO_2 membrane using a FIB. The nanopore diameter was then shrunk by using thermal heat in a nitrogen ambient. Expansion in the nanopore size was also observed in some cases, similar to previous reports.[17] The silicon dioxide was annealed during thermal treatment and changed the nanopore size. It was hypothesized that the process was driven by an overall reduction in surface energy of the nanopore periphery and surrounding area. The previous work also determined that when the diameter of the pore was less than the thickness of the membrane, the nanopore shrank but if the diameter of the pore was greater than the thickness of the membrane, the pore expanded.[16] Four temperatures were used to test the shrinking process: 900 °C, 1075 °C, 1150 °C, and 1250 °C. The 900 °C temperature produced no shrinking while the 1250 °C temperature produced excessive thermal stresses. The results of the 1075 and 1150 °C data are shown in Table I.[16] These results show a distinct behavior for the shrinking nanopore where the rate of shrinking is much faster at higher temperature. The focus of this work is to determine what factors control the shrinking of a nanopore in a membrane when the diameter of the pore is less than the membrane thickness.

The direct thermal heating method has several advantages in comparison to electron beam (e-beam) microscope based shrinking or drilling approaches. For example, the direct thermal heating batch-shrinks multiple nanopores in

TABLE I. Average radius of thermally shrinking SiO_2 nanopores at specific times at two temperatures in a furnace (from Ref. 16).

1075 °C		1150 °C	
Time (s)	Radius (nm)	Time (s)	Radius (nm)
0	115	0	127
300	90	300	75
600	52.5	600	10
900	17.5	642	1.5
1020	0		

a)Author to whom correspondence should be addressed. Electronic mail: SMIQBAL@uta.edu. Telephone: +1-817-272-0228.

parallel, whereas the e-beam approach processes one nanopore at a time. Also, unlike e-beam induced shrinking/drilling, the direct thermal heating does not result in chemical composition variation on the nanopore surface.

A sufficient theoretical model does not exist to allow the precise fabrication of predetermined nanopore sizes. A model which could be adapted to solve this problem was reported for an experiment involving the change in hole size for monocrystalline thin films of gold.[18] This model requires values for viscosity and its self-surface diffusion coefficient. In this work, we solve this by using the viscosity model for 100% fused silica glass and then curve-fitting to the data in Table I to find the self-surface diffusion coefficient. A closed-form solution can then be given to define exact conditions for precise nanopore shrinking.

In order to model how a SiO_2 nanopore shrinks at a given temperature, the first step is to discover its viscosity at said temperature. For this, the Vogel-Fulcher-Tammann (VFT) equation was used. VFT equation is used for modeling the viscosity of different types of glass. The VFT equation is accurate for temperatures of a few thousand centigrades, which covers the temperatures at which SiO_2 nanopore shrinks ($\sim$1000–1200 °C).[16,19] The VFT equation is given as follows where η is viscosity, T is temperature, and A, B, and T_0 are physical parameters inherent to the glass.[20]

$$\mathrm{Log}_{10}(\eta) = A + \frac{B}{T - T_0}. \tag{1}$$

The VFT equation data for fused silica glass is given in Table II.[20] The fused silica glass consists of 100% amorphous SiO_2. In lieu of viscosity data for wafer-grown SiO_2, the glass framework is a close approximation and thus this data were used. Furthermore, wafer-grown SiO_2 with ordered structure could be reflowed to make it amorphous.

Partially liquefied thin films with holes in them show a phenomenon where the holes are inclined to expand or shrink depending on the ratio of the initial diameter to the initial film thickness.[21] If the diameter is less than the thickness, the hole will shrink. This is based on the surface free energy of the thin film as a function of surface tension and the area.[16,21,22] The area is obtained by modeling the pore as a cylindrical hole with the change in surface energy calculated from:[16]

$$\Delta E = \gamma 2\pi(rh - r^2), \tag{2}$$

where γ is viscosity (in Pa s), r is the pore radius, h is the pore depth or membrane thickness, and ΔE is the change in surface free energy. The criterion for pore shrinking is defined as $2r < h$. Note that the change from η to γ in representing viscosity denotes a conversion of units from dPa-s to Pa-s.

TABLE II. Parameters and units for the VFT equation and their values for fused silica glass.[20]

Parameter	Value	Unit
η		dPa-s
T		°C
A	−7.9250	No unit
B	31282.9	°C
T_0	−415	°C

The pore's surface tension acts to give normalizing forces that resist the expansion or shrinking of the pore. As such, it can be said that there is a pressure P exerted throughout the surface area of the pore. From this, it can be conceived that the change in surface free energy with respect to the change in radius describes this pressure as the mass flow rate per area (with units of kg/s per square-meter). This is corroborated by previous work by Lanxner *et al.*[18] Substituting Eq. (1) into this relation gives the following equation:

$$P = \frac{\Delta E}{(-2\pi r h \Delta r)} = \gamma\left(\frac{2}{h} - \frac{1}{r}\right). \tag{3}$$

The flux of the membrane's molecules is given by a mobility coefficient M (Eq. (4)), where N is the number of molecules per unit volume, D_s is the self-surface diffusion coefficient of SiO_2, T is the temperature (in K), and k is the Boltzmann constant. The product of P and M (Eq. (5)) describes the change in pore radius with respect to time.[18] This can then be rearranged to the form of Eq. (6) which is then integrated to get a closed form of the relation depicting the pore size dependence on time for shrinking at specific temperatures.

$$M = \frac{4(\mathrm{N}^{-1/3})^4 \mathrm{D_s}}{h^2 kT}, \tag{4}$$

$$\frac{dr}{dt} = PM = \left[\frac{2}{h} - \frac{1}{r}\right]\frac{4(\mathrm{N}^{-1/3})^4 \mathrm{D_s}\gamma}{h^2 kT}, \tag{5}$$

$$\frac{h^2 kT}{4(\mathrm{N}^{-1/3})^4 \mathrm{D_s}\gamma} \times \frac{1}{\left[\frac{2}{h} - \frac{1}{r}\right]} dr = dt. \tag{6}$$

Integrating Eq. (6) with initial pore radius r_0, with desired pore radius r meters and initial $t = 0$ seconds gives the general relation as:

$$t = \frac{h^3 kT}{16 D_s \gamma N^{-\frac{4}{3}}}\left[2(r - r_o) + h\,\mathrm{Log}_e\left(\frac{|2r - h|}{|2r_o - h|}\right)\right]. \tag{7}$$

The parameter N can be calculated based on the density of SiO_2. However, it must be taken into account that the molecular density would change based on the temperature of the process, in contrast to the constant value assumed at room temperature. Therefore, the density at temperature T must first be derived with the thermal expansion equation below:

$$\frac{d}{1 + \beta(T - 20\,^\circ\mathrm{C})} = d_T, \tag{8}$$

where d is the density of SiO_2 at room temperature ($\sim$2 648 000 g/m^3), β is the volumetric thermal expansion coefficient for SiO_2 ($\sim 15 \times 10^{-7}$/°C), and d_T is the density of SiO_2 at temperature T. The parameter N can be thus calculated by dividing d_T by the molar mass of SiO_2 then multiplying with Avogadro's number.

Equation (1) can be used to calculate viscosity (γ) during experiments using values from Table II.[16] At 1075 and 1150 °C, we get γ of 1.176×10^{14} and 1.159×10^{13} Pa s,

respectively. Using these values, and for $h = 300$ nm, Eq. (2) can be used to see ΔE as dependent on r. The plots for the two temperatures are shown in Fig. 1.

Examination of these plots show that $\Delta E = 0$ when $r = 0$ and $r = h$, and that there is a maxima at the point where $r = 0.5\,h$. This shows that when the radius is zero, the pore having closed completely, the surface free energy reaches its minimum and does not decrease further. The maximum represents the border between the pore shrinking and the pore expanding. This maximum is theoretically stable, but real-world ambient conditions cause a diversion to the left or to the right from this point. The curve to the left of the maximum shows the pore shrinking. The curve to the right of the maximum shows the pore expanding. The point $r = h$ shows where the pore expands to its maximum diameter, the surface free energy here again reaches its minimum and no longer decreases.

The mass flow can be also calculated using Table II data and Eq. (3). The inset to Fig. 1 shows that when the nanopore shrinks to a radius below 10 nm, the rate of the movement of mass to fill and shrink the pore increases in magnitude asymptotically. On the other hand, when the pore is expanding it shows that the magnitude of the movement rate of mass decreases asymptotically. This supports the notion that controllably shrinking a nanopore to a specific size becomes more difficult below 10 nm. At the same time, expanding it becomes easier to control the bigger it becomes.

The only unknown left to account for in Eq. (7) is the value for D_s, the self-surface diffusion coefficient. In simple treatment of mass flow, D_s is used as a proportionality constant. However, here the issue of diffusion is a more involved one. We believe that the D_s is not constant but is a function of the potential gradient stemming from fluidic inclination to reduced free energy, which in turn is a function of nanopore radius. Thus, D_s can be found by entering all relevant values into the equation and using the radius and time values at a given temperature from Table I to tabulate discrete data points for D_s as a function of radius. Take note that D_s cannot be extracted for $r = r_0$. This is done for both 1075 °C and 1150 °C, and then theoretical curves are fit to the extracted data points (shown in Fig. 2). The simplest and most accurate curve fit is a first-order polynomial fit for both instances. The mean squared errors between the theoretical and extracted experimental data points for 1075 and 1150 °C were 3.5×10^{-182} and 1.3×10^{-180} m^2/s, respectively.

By using the correct value of D_s with its corresponding r value based on the curves in Fig. 2, it becomes possible now to calculate and plot the shrinking time t as a function of r for the two temperatures. The plots for both are shown in the inset to Fig. 2. It should be noted here that by properly curve-fitting D_s, the theoretical curve for the nanopore shrinking rate also fits well to the experimental data. The mean squared errors between the theoretical and pre-existing experimental data points were 3.6 nm for 1075°C and 0.3 nm for 1150 °C.

The theoretical curves shown in the inset to Fig. 2 match the experimental data quite well. However, the following caveats should be pointed out. When using a set of experimental data wherein the final data point shows the pore radius at zero (such as the 1075 °C data in Table I), it is impossible to tell if that final data point was taken exactly when the pore closed. The exception is if one were to be able to observe and record such an event in real-time during the shrinking process. This was not so for the Table I data. With this in mind, the only choice is to discard the final data point when considering the curve-fitting for D_s value. With no data points near where $r = 0$, the theoretical curve's prediction (see Fig. 2 inset) is slightly higher in this area and is reflected in its higher mean square error. Contrasting this is the 1150 °C plot in inset to Fig. 2, which does not have this issue.

With all the unknowns accounted for, it is now possible to generate hypothetical pore-size vs. temperature curves based on differing values of pore membrane thickness. Fig. 3 shows theoretical curves for 1150 °C and 1075 (inset) where the hypothetical membrane thicknesses are 400, 600, 800, and 1000 nm. The trend shows that the overall slope of the curve decreases as membrane thickness increases, suggesting

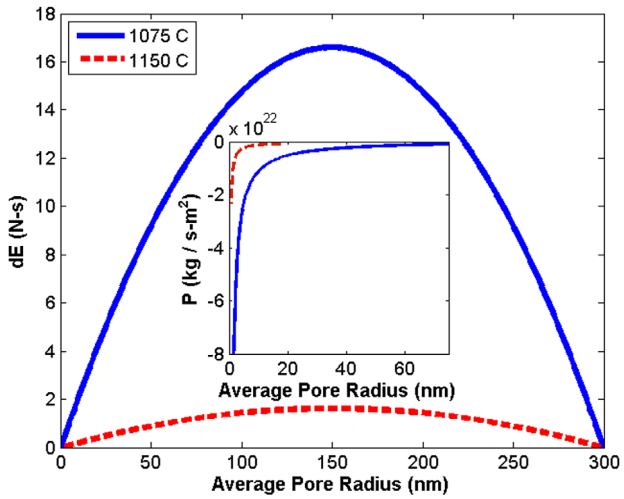

FIG. 1. Change in surface free energy with respect to nanopore radius for 1075 and 1150 °C. $\Delta E = 0$ and $r = 0$ and $r = h$ with maxima at $r = 0.5\,h$. To the left of the maxima the nanopore shrinks and it expands to the right. The inset depicts mass flow rate per area with respect to pore radius for 1075 °C and 1150 °C. Past the 10 nm point, shrinking pores asymptotically increase in mass flow rate magnitude while expanding pores decrease asymptotically.

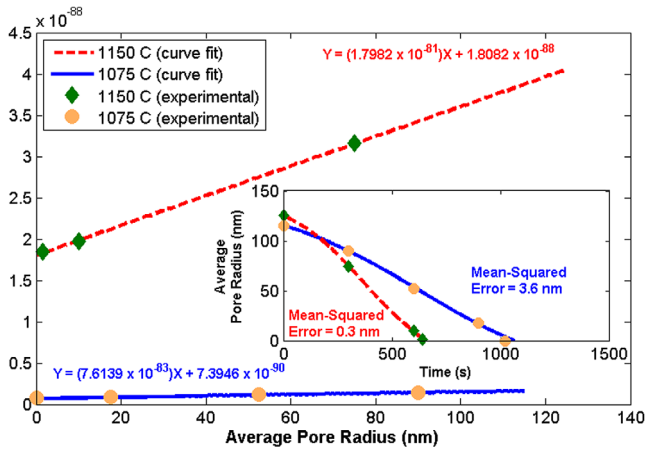

FIG. 2. Self-surface diffusion coefficient with respect to nanopore radius for 1075 °C and 1150 °C. The dot-markers are the extracted data points while the line shows the curve-fit. The inset shows pore radius shrinking with respect to time for 1075 °C and 1150 °C. The dot-markers are the experimental data points while the lines show the theoretical curves predicted by Eq. (7).

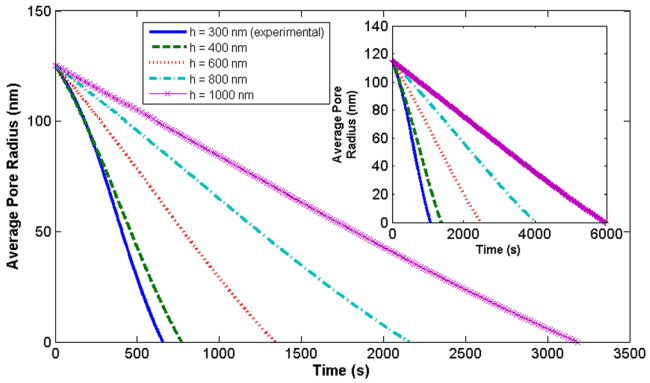

FIG. 3. Pore radius shrinking with respect to time at 1150 °C (inset: for 1075 °C) for several hypothetical values of pore membrane thickness h. The original, experimental value of h is included for comparison.

an inversely proportional relationship. Furthermore, this relationship predicts that increasing membrane thickness will also increase the amount of time it takes for the pore to shrink to its closing point. Thus, increasing the membrane thickness can provide much more control to accurately achieve the final diameter of the nanopore.

This article presents a model that captures essential details of nanopore thermal shrinking process. The effects of temperature on the viscosity of the silicon dioxide film show a direct effect on whether the nanopore shrinks or expands. The exact solution to the diffusion coefficient of silicon dioxide provides a first order fit to the experimental data. This work provides useful control of process parameter choices for nanopore fabrication in parallel.

The research conducted in this work was supported by grants from The Metroplex Research Consortium for Electronic Devices and Materials (MCREDM), Arlington, Texas, and by National Science Foundation Grants CAREER ECCS-0845669 and ECCS-1201878.

[1]M. Firnkes, D. Pedone, J. Knezevic, M. Döblinger, and U. Rant, Nano Lett. **10**, 2162–2167 (2010).
[2]H. Chang, B. M. Venkatesan, S. M. Iqbal, G. Andreadakis, F. Kosari, G. Vasmatzis, D. Peroulis, and R. Bashir, Biomed. Microdevices **8**, 263–269 (2006).
[3]S. M. Iqbal, D. Akin, and R. Bashir, Nat. Nanotechnol. **2**, 243–248 (2007).
[4]A. Ramachandran, Y. Liu, W. Asghar, and S. M. Iqbal, Am. J. Biomed. Sci. **1**, 344–351 (2009).
[5]A. Singer, M. Wanunu, W. Morrison, H. Kuhn, M. Frank-Kamenetskii, and A. Meller, Nano Lett. **10**, 738–742 (2010).
[6]B. M. Venkatesan, A. B. Shah, J.-M. Zuo, and R. Bashir, Adv. Funct. Mater. **20**, 1266–1275 (2010).
[7]D. Fologea, M. Gershow, B. Ledden, D. S. McNabb, J. A. Golovchenko, and J. Li, Nano Lett. **5**, 1905–1909 (2005).
[8]R. M. M. Smeets, U. F. Keyser, D. Krapf, M. Y. Wu, N. H. Dekker, and C. Dekker, Nano Lett. **6**, 89–95 (2006).
[9]S. M. Iqbal and R. Bashir, *Nanopores: Sensing and Fundamental Biological Interactions* (Springer, 2011).
[10]H. Chang, S. M. Iqbal, E. A. Stach, A. H. King, N. J. Zaluzec, and R. Bashir, Appl. Phys. Lett. **88**, 103109 (2006).
[11]C. J. Lo, T. Aref, and A. Bezryadin, Nanotechnology **17**, 3264 (2006).
[12]S. R. Park, H. Peng, and X. S. Ling, Small **3**, 116–119 (2007).
[13]A. J. Storm, J. H. Chen, X. S. Ling, H. W. Zandbergen, and C. Dekker, Nature Mater. **2**, 537–540 (2003).
[14]S. Wu, S. R. Park, and X. S. Ling, Nano Lett. **6**, 2571–2576 (2006).
[15]B. M. Venkatesan and R. Bashir, Nat. Nanotechnol. **6**, 615–624 (2011).
[16]W. Asghar, A. Ilyas, J. A. Billo, and S. M. Iqbal, Nanoscale Res. Lett. **6**, 372 (2011).
[17]A. J. Storm, J. H. Chen, X. S. Ling, H. W. Zandbergen, and C. Dekker, J. Appl. Phys. **98**, 014307 (2005).
[18]M. Lanxner, C. L. Bauer, and R. Scholz, J. Vac. Sci. Technol. A **5**, 1748–1749 (1987).
[19]H. Mehrer, *Diffusion in Solids: Fundamentals, Methods, Materials, Diffusion-Controlled Processes*. (Springer, 2007).
[20]W. Martienssen and H. Warlimont, *Springer Handbook of Condensed Matter and Materials Data* (Springer, 2005).
[21]G. I. Taylor and D. H. Michael, J. Fluid Mech. **58**, 625–639 (1973).
[22]F. Behroozi, Eur. J. Phys. **31**, L31 (2010).